

STRUCTURAL FORMS OF FLUORIDES IN BONE TISSUE OF ANIMALS UNDER CHRONIC FLUORIDE INTOXICATION

S. P. Gabuda,¹ A. A. Gaidash,¹ S. G. Kozlova,¹
and N. L. Allan²

UDC 546.7.731;572.43;572.33

High-resolution solid-state ¹⁹F NMR method has been used to examine the chemical structural forms of fluorine introduced into the bone tissue of experimental animals (Vistar rats) exposed to 30 day fluoride inhalation. It is shown that in the bone tissue three structural forms of fluorides are deposited: a solid phase of F-apatite and mobile nanoparticles of CaF₂ and MgF₂ (or KMgF₃) with the ratio of fluorine concentration in these three forms ~2:2:1. During the following 30 day rehabilitation this ratio remains constant, the total fluorine content in the bone tissue decreases ~3 times and the F-apatite phase transforms into disordered (F, OH)-apatite. A protective effect of the zeolitic enterosorbent (klinoptilolite) on fluorine binding in the intoxication process was found, as well as the promotional effect of this enterosorbent on fluorine excretion during the postfluoride rehabilitation.

Keywords: bone tissue of animals, fluoride intoxication, fluorides, nuclear magnetic resonance spectra.

INTRODUCTION

The average content of fluorine in soil is $\sim 2 \cdot 10^{-4}$ and in living organisms is $\sim 10^{-6}$ by the weight. According to numerous investigations [1], a small content of fluorine in organisms is usual and due to its dental caries-protection effect on bone tissue and dental enamel [2]. Fluorine salts are also commonly used in clinical practice as active components in treatments for osteoporosis [3]. However excess fluorine intake may cause fluorosis [1, 4], the endemic disease which is widespread in dry regions where the groundwater and deep-well water with increased fluorine content is used for drinking and watering [5, 6]. Fluorosis can also result from respiratory (inhalation) intoxication due to the admixture of hydrogen fluoride vapors in the air close to surface mining, during aluminum smelting, etc. [7]. Currently there is considerable discussion of fluorosis risks associated with the wide use of admittedly inert fluorine-carbon compounds into household appliances, with the fluoridation of drinking water, and with the active use of anticariogenic tooth-pastes [8]. This has stimulated a sharp increase in public interest in the problems of fluoride intoxication [9].

The main difficulty is the diagnosis of fluorosis, whose manifestations and symptoms may resemble such common diseases as osteoarthritis, rheumatism, spondylosis, renal osteodystrophy, osteopetrosis, diffuse idiopathic skeletal hyperostosis, and so on [1, 4]. Since the X-ray scattering factors of fluorine and oxygen are so similar, the potential for radiological methods of investigation here is severely limited. Thus direct methods for the investigation of fluoride compounds in bone tissue are of fundamental interest. These methods are based on fluorine nucleus magnetic resonance (¹⁹F NMR) which permits qualitative and quantitative identification of fluorine in different materials [10], including bone tissue

¹A. V. Nikolaev Institute of Inorganic Chemistry, Siberian Division, Russian Academy of Sciences, Novosibirsk; gabuda@che.nsk.su. ²School of Chemistry, University of Bristol, Cantock's Close, Bristol BS8 1TS, U. K. Translated from *Zhurnal Strukturnoi Khimii*, Vol. 47, No.2, pp. 264-272, March-April, 2006. Original article submitted May 5, 2005.

identification of the deposited fluorine compounds, and their spatial and time dynamics. ^{19}F NMR is thus an important addition to traditional X-ray and X-ray diffraction methods both in molecular biological investigations and medical diagnostics, where the methods of computed NMR tomography supplement present methods of computed X-ray tomography.

The purpose of this work is the use of ^{19}F NMR to investigate the structural forms of fluorides in the bone tissue of experimental animals who were protractedly subjected to fluoride intoxication via weak (lower than MPC) inhalation. Quantitative data on these fluorides may elucidate their possible role in the mechanisms of fluorine transport into bone tissue under chronic intake from the environment and in the mechanisms of fluorine washout from bone tissue and from organisms during the rehabilitation process. One of the aims of this work is the investigation of the possibility to use zeolitic enterosorbents as protectors from fluoride intoxication — for sorption of fluorides in the gastrointestinal tract and for prevention (or inhibition) of fluoride inflowing into the bloodstream. Zeolites are a new class of enterosorbents with pronounced immunopotentiating activity [12]. We discuss the problem of how zeolitic enterosorbents interact chemically with fluorides under the complex conditions present in organisms, and also problems associated with the quantitative assessment of their prophylactic or therapeutic effects on fluoride intoxication.

INVESTIGATION PROCEDURE

Experimental animals and mineral food supplements. Male Vistar rats were used as experimental animals. Animals were kept under usual conditions: light/dark rhythm 12/12 h, temperature 22°C, humidity 55%. Balanced diet included a humid mush from dry corn mix, fresh vegetables, and standard combined feed granules. The mush was prepared using the following components: wheat, pearl-barley, and oatmeal in the ratio 1:1:1 with the addition of bread crackers, sunflower-seed oil, and fish oil concentrate. The total weight of daily ration varied within the limits of 20% of animal body weight.

Zeolitic food supplement was prepared by fine grinding of klinoptilolite-containing zeolitic tuff from Kholinskoe field (Transbaikalia). According to chemical analysis data, the obtained sorbent contained approximately 75 wt.% of klinoptilolite with the idealized formula $\text{CaNa}_2\text{K}_2[\text{Al}_6\text{Si}_{30}\text{O}_{72}]\cdot 24\text{H}_2\text{O}$ (which we abbreviate to CaZ, where $Z = \{\text{Na}_2\text{K}_2[\text{Al}_6\text{Si}_{30}\text{O}_{72}]\cdot 24\text{H}_2\text{O}\}^{2-}$). The remaining 25% are represented by montmorillonite, feldspars, micas, and quartz. The average size of powder particles is about 30-40 μm ; the prepared enterosorbent was calcined at 180°C and added into the feed of a given fraction of the animals in a dosage of 0.3-0.5% of daily humid mush ration.

Sample preparation. The experimental animals were exposed on working floors in the electrolysis workshops of Krasnoyarsk Aluminum Plant (KrAP) in summer-autumn periods (August-October) in the period 1995-1999. According to the data of everyday control for the working zone, the air temperature was maintained between 22-24°C, the concentration of hydrogen fluoride in the atmosphere of the workshops varying between 0.2-0.6 mg/m^3 (about 0.1-0.3 MPC). To minimise possible effects from magnetic fields affecting the animals, the cages were placed at a distance of 15-20 m from conducting buses. The adaptation of animals to habitation conditions in the workshops involved successive increases in exposure time — during the first two weeks the exposure time was successively 2 h, 4 h, 6 h, and 12 h a day. Then it was round-the-clock from three weeks to 1 month. To analyze more long-term intoxication effects one group of animals was left on the working floors in the electrolysis workshops for 2.5-3.5 months.

The experimental animals were divided into 4 groups with 4 animals in each. Group 1 was composed from the animals subjected to fluoride intoxication, standard feed. Group 2 was formed from the animals subjected to fluoride intoxication, standard feed with the addition of the zeolitic enterosorbents. Group 3 was formed from animals subjected to fluoride intoxication followed by a month of rehabilitation, standard feed. Group 4 was formed from the animals subjected to fluoride intoxication followed by a month of rehabilitation, standard feed with the addition of the zeolitic enterosorbents. After each cycle was completed, samples of femoral bones of animals ($\sim 2 \times 3 \times 5 \text{ mm}^3$) were taken to carry out elemental analysis.

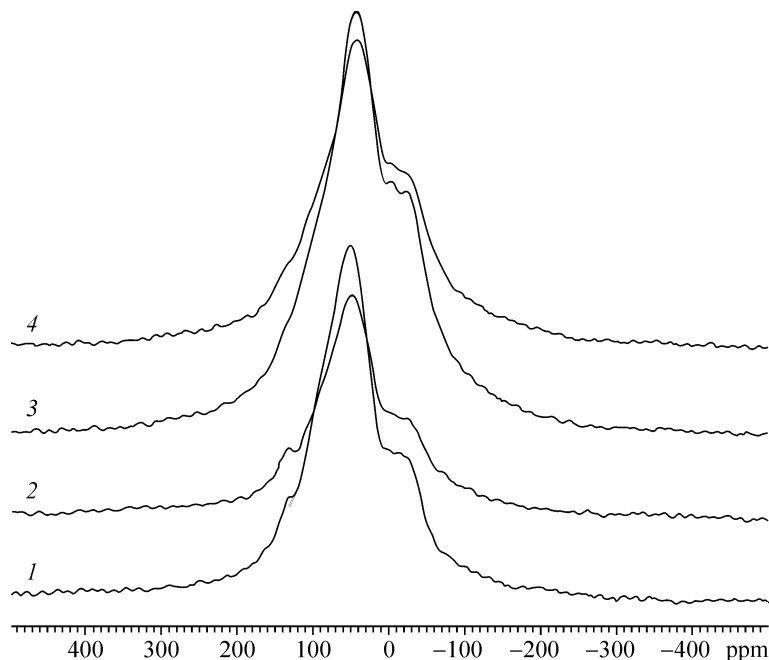


Fig. 1. ^{19}F NMR experimental spectra of four samples of rat's femoral bone; $B_0 = 7$ T; standard is C_6F_6 . Notations: 1 — inhalation F-intoxication, standard feed with addition of the zeolitic food supplement; 2 — inhalation F-intoxication, standard feed; 3 — postfluoride rehabilitation (1 month), standard feed with addition of the zeolitic food supplement; 4 — postfluoride rehabilitation (1 month), standard feed.

The value of the mineral part of the bone was found to be ~50% by the weight, and in all cases the P/Ca ratio in the bone is slightly reduced relative to that of apatite. This indicates some calcium deficiency in the bone tissue.

^{19}F NMR-measurements. For NMR-investigations, the samples were reduced to fine particles; ^{19}F NMR spectra were recorded on a pulsed spectrometer Bruker CXP-300, magnetic field $B_0 = 7$ T, Larmor frequency $\nu_0 = 284.4$ MHz. Hexafluorobenzene, C_6F_6 , was used as the liquid standards (the shift in relation to F_2 is 589 ± 2 ppm towards the strong field [10]). Specific ^{19}F NMR spectra of intact samples of femoral bones from groups 1-4 are shown in Fig. 1. We have also recorded ^{19}F NMR spectra for powder samples of natural apatite ($\text{F}_x(\text{OH})_{1-x}$) with $x \approx 0.2$ from the Slyudianka field (lake Baikal region) and CaF_2 and MgF_2 reagents of analytical grade in comparative purposes.

Quantitative analysis of fluorine binding effects in the bone tissue has been performed on the basis of recording of NMR spectra in the magnetic field $B_0 = 0.55$ T whereby spectral components are not practically resolved. The principles of the analysis of the spectra have been described earlier [13, 14]. We carried out a quantitative comparison of the integrated intensities of ^{19}F NMR signals for the samples of the bone tissue from the experimental animals under different conditions of fluoride intoxication. The sample weights were determined to an accuracy of ± 1 mg, and the recording of NMR spectra of the bone tissue and the standard standard carried out under identical conditions. Owing to a high level of instrumental noise, the accuracy of the integrated intensities of ^{19}F NMR signals and the fluorine content was about $\pm 10\%$.

EXPERIMENTAL RESULTS

Qualitative analysis of ^{19}F NMR spectra of bone tissue. Fig. 1 depicts the obtained ^{19}F NMR spectra of the bone tissue. For comparison, Fig. 2 illustrates the spectrum of polycrystalline apatite ($\text{F}_x(\text{OH})_{1-x}$), and Fig. 3 displays the spectrum of polycrystalline F-apatite (using the data from [15]). For ease of comparison of the effects associated with different

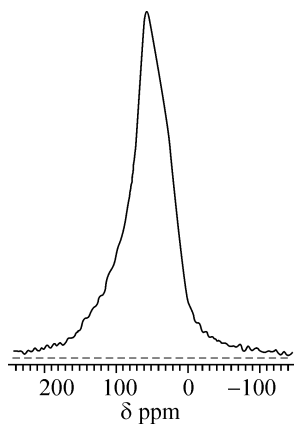


Fig. 2. ^{19}F NMR experimental spectrum of natural apatite sample of $\text{Ca}_5(\text{PO}_4)_3[\text{F}_{0.1}(\text{OH})_{0.9}]$ composition; $B_0 = 7$ T; standard is C_6F_6 .

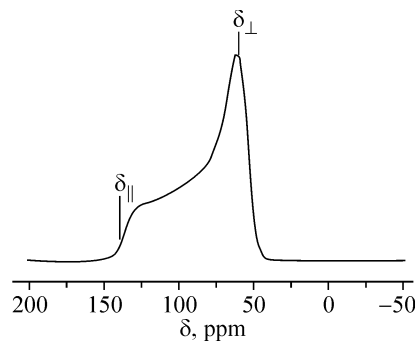


Fig. 3. Form of ^{19}F NMR spectrum of polycrystalline apatite according to the data from [15].

conditions affecting the preparation of samples, all curves are located on the same scale of chemical shifts (CS) where the CS value for C_6F_6 is taken as a secondary standard. The band structure in the spectra (Fig. 1) can be divided into three parts:

1) the area associated with weak magnetic fields (150-100 ppm). There is an evident anomaly near 140-150 ppm for samples 1 and 2 that were obtained under the conditions of strong fluoride intoxication. This anomaly coincides with the position of feature in the ^{19}F NMR spectrum for F-apatite at 140 ppm corresponding to a longitudinal component of the chemical shift tensor $\delta_{||}$ for F-apatite [15]. This result unambiguously indicates that in the process of fluorine binding in bone tissue the equilibrium is shifted towards a strictly ordered formation of F^- ion chains which is typical for pure F-apatite.

On the other hand, for samples 3 and 4, obtained from animals undergoing different postfluoride rehabilitation stages, such anomalies in 100-150 ppm area are virtually absent. This feature makes the ^{19}F NMR spectra for samples 3 and 4 more similar to NMR spectra for a natural apatite sample (see Fig. 2) that contains an admixture of OH-groups (10-20% from the number of structural positions for monovalent anions in apatite). Thus we conclude that in the rehabilitation process a shift of the equilibrium conditions takes place such that a disordered distribution of fluoride and hydroxide ions in monovalent anion chains is preferred;

2) the most intense central parts of the ^{19}F NMR spectra within the interval 100-0 ppm differ considerably both in shape and width from the asymmetrical peak for natural F-apatite. As will be explored later, a possible cause of the observed difference in peak shapes in bone tissue and natural apatite spectra could be the presence of fluorite CaF_2 . The main argument supporting this hypothesis is the value of the chemical shift of fluorite $\langle\delta(\text{CaF}_2)\rangle = 55$ ppm [15] that practically coincides with the position of the orthogonal component δ_{\perp} of the CS tensor for ^{19}F NMR apatite. Indirect support also comes from Raman spectra which demonstrate the presence of absorption bands that are typical of CaF_2 (unpublished data);

3) the range from ~ 0 ppm to ~ -100 ppm, where the ^{19}F NMR spectra of F-apatite and bone tissue differ most markedly. In natural apatite, there are practically no peaks in this interval. The presence of ^{19}F NMR-absorption for the bone tissue in this range can be explained by the additional presence of a specific fluoride. MgF_2 (found in nature as sellaite) is one possibility. The average value of the ^{19}F NMR chemical shift for magnesium difluoride (sellaite) is $\langle\delta(\text{MgF}_2)\rangle = -27 \pm 1$ ppm [15]; similar values are noticed for the perovskites KMgF_3 ($\delta = -15.5$ ppm [16]) and NaMgF_3 ($\delta = -32.5$ ppm [16]).

Quantitative analysis of the spectral shape for ^{19}F NMR. The NMR spectra of polycrystals are the sum of NMR signals for separate chaotically oriented small crystals. The envelope for these signals is some curve whose parameters are related to the angular dependence of the chemical shift δ . The method to determine the CS parameters follows from the

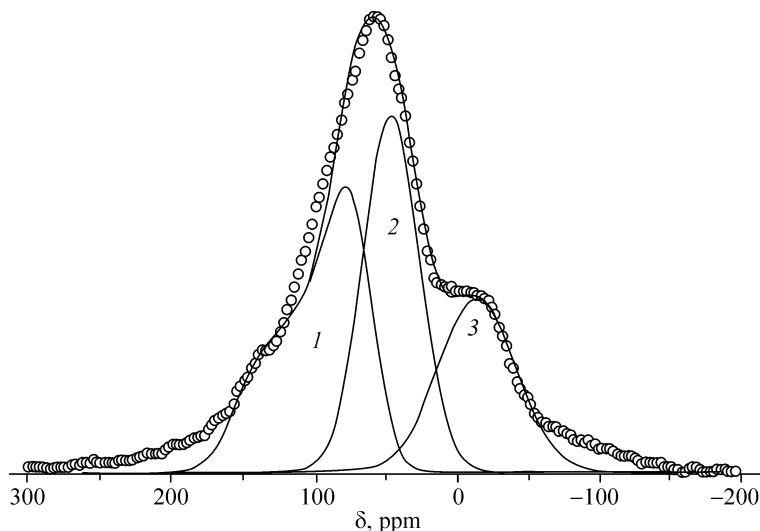


Fig. 4. Decomposition into components of the central part of ^{19}F NMR spectrum of rat's femoral bone: 1 — F-apatite (40% of the area); 2 — CaF_2 (36% of the area; $\beta^2 = 1.9 \text{ G}$; $\langle\delta\rangle = +45 \text{ ppm}$); 3 — MgF_2 (24% of the area; $\beta^2 = 3.6 \text{ G}$; $\langle\delta\rangle = -17 \text{ ppm}$). The envelope (thin curve) is the sum of these three components; the punctual curve (circles) is the experimental spectrum of sample 1; $B_0 = 7 \text{ T}$; standard is C_6F_6 .

results of the envelope shape calculation [10, 15]:

$$f(\delta) = \int g(\langle\delta\rangle - \delta) S(\delta - \langle\delta\rangle) d\delta,$$

where $\langle\delta\rangle$ is an isotropic component of the chemical shift. The function $g(\langle\delta\rangle - \delta)$ describes the effect of chemical shift anisotropy:

$$g(\langle\delta\rangle - \delta) = \text{const} [1 + (\langle\delta\rangle - \delta)/\alpha]^{-1/2},$$

and the function $S(\delta - \langle\delta\rangle)$ is a so-called broadening factor related to the shape of a NMR spectral line of a monocrystal. This form is assumed to be of Gaussian form:

$$S(\delta - \langle\delta\rangle) = \exp[-(\delta - \langle\delta\rangle)^2 / 2\beta^2] / \beta \sqrt{2\pi},$$

where β is a parameter of the NMR line shape. It is approximately equal to half-width of the NMR spectral line for a monocrystal. To calculate values of δ_{\parallel} and δ_{\perp} , parameters were taken from the literature [15], $\langle\delta\rangle = 1/3(\delta_{\parallel} + 2\delta_{\perp})$, and $\alpha = -1/3(\delta_{\parallel} - \delta_{\perp})$. Fig. 4 illustrates the results of an optimal "fitting" of this curve to ^{19}F NMR spectra of bone tissue using sample 2 as an example. It is seen that the width of the calculated asymmetrical spectral band in the ^{19}F NMR spectra of F-apatite is less than a half of that in the observed spectrum. In attempting our quantitative analysis we have therefore also used existing data for the curve shapes of other possible (practically insoluble) structural forms of fluorides in bone tissue — fluorite CaF_2 and sellaite MgF_2 .

To simplify the calculation we approximated the shape of ^{19}F NMR spectra for the possible impurity components as Gaussian distributions using the experimental values of $\beta(\text{CaF}_2)$ and $\beta(\text{MgF}_2)$. First, we tried to reproduce the experimental spectrum as the sum of the spectra of three given components with only two variable parameters — the relative concentrations of CaF_2 and MgF_2 . However, this simplest approximation failed to give an acceptable description of the observed shape of the spectrum. So a more complex model was used, with two additional variable parameters — the values of β which govern the width of the signals of CaF_2 and MgF_2 when present in the mixture. Physically this means we allow for the possibility of mobility of these species in bond tissue, since this governs the width of the signals. The best agreement of the theoretical absorption curve with experiment for all four curves (see Fig. 1) was obtained with a ratio of fluorine signal intensity from apatite to those from CaF_2 and from MgF_2 of 2:2:1 respectively. Fig. 4 illustrates the results of the optimal approximation for

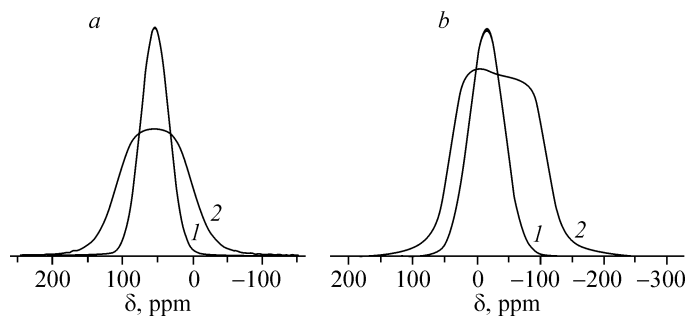


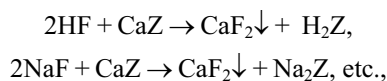
Fig. 5. ^{19}F NMR spectra components related to CaF_2 (a) and MgF_2 (b) in bone tissue (curves 1) compared with the ^{19}F NMR experimental spectra of CaF_2 and MgF_2 powders (curves 2). $B_0 = 7 \text{ T}$ (100 ppm = 7 G); standard is C_6F_6 .

the ^{19}F NMR spectrum of sample 2.

The comparison of the theoretical curve with experiment shows satisfactory agreement with two exceptions. The first of these concerns the interval 80-120 ppm. The observed lack of coincidence of the theoretical and experimental curves may indicate the presence of an (F, OH)-apatite admixture whose ^{19}F NMR signal falls in the interval 70-105 ppm. However, given the present accuracy of the intensity measurements of the NMR spectra ($\sim 10\%$), unambiguous extraction of a given signal is difficult.

The second difficulty concerns the character of NMR spectral lines related to CaF_2 and MgF_2 fluorides in bone tissue. Fig. 5a and b illustrate the components of ^{19}F NMR spectra of bone tissue that are assigned to CaF_2 and MgF_2 compared with the spectra of polycrystalline CaF_2 and MgF_2 obtained under the same conditions. CaF_2 and MgF_2 samples in the form of white colored powder were analytical grade reagents produced by the “Chimreaktiv.” It is evident that the strong-field line in the interval ~ 50 ppm to -100 ppm is shifted towards the weak field with respect to the center of gravity of the experimental ^{19}F NMR spectrum of MgF_2 powder (Fig. 5b). This suggests an assignment of the strong-field line in the ^{19}F NMR spectrum for bone tissue to perovskite KMgF_3 . Since the dipole broadening in the ^{19}F NMR spectra of KMgF_3 is close to that for MgF_2 , we see that the observed ^{19}F NMR spectral bands of CaF_2 and MgF_2 in bone tissue are about two times narrower than the corresponding bands for the polycrystalline samples. Thus CaF_2 and MgF_2 (or KMgF_3) particles in bone tissue are characterized by uniaxial rotational diffusion which halves the width of NMR lines and quarters the root-mean-square width [10, 15]. For more general rotational diffusion, such as isotropic rotation, there is complete averaging of the dipole spectrum width and there is a transition to liquid-like NMR spectra. This transition is not observed in our ^{19}F NMR spectra for bone tissue, supporting uniaxial rotational diffusion of CaF_2 and MgF_2 particles. The unusual mechanism of the rotational diffusion in this case can be related to the appearance of an insulating layer of organic substances on the surface of nanoparticles that is typical of well-known flotation mechanisms.

The dynamics of fluorine binding in bone tissue. Fig. 6 shows the comparison of spectra recorded under similar conditions and scaled to the same weight of the sample. Fluorine sorption in bone tissue is seen to considerably diminish when zeolitic food supplements are used in animal feed. Fig. 7 summarizes the results of the analysis. The protective effect of the zeolitic food supplements that decrease the fluorine intake into bone tissue (under conditions of fluoride intoxication) is evident. A possible mechanism for the protective effect of zeolites is the result of fluorine binding in the bowels according to the ion exchange reactions:



where Z is zeolite. It is more difficult to suggest an acceleration mechanism of fluorine washout from bone tissue during the postfluoride rehabilitation when fluorine is present as sparingly soluble compounds — fluorineapatite and CaF_2 and MgF_2

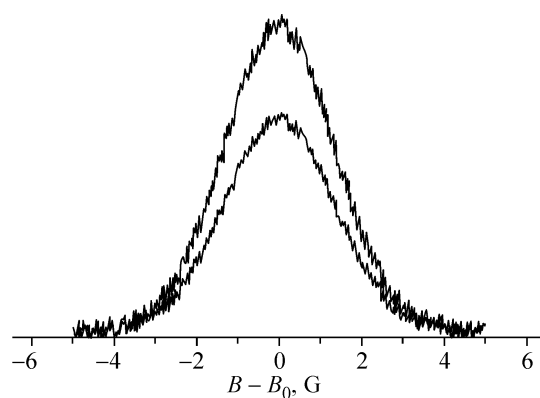


Fig. 6. Protective effect of klinoptilolite under fluoride intoxication conditions. Upper curve: ^{19}F NMR spectrum of rat's femoral bone exposed in the electrolysis workshop (2.5 months, standard feed). The lower curve is the same for rats fed with zeolitic food supplement. The spectra recording conditions: $B_0 = 5500$ G, spectral components are not resolved (1 G = 90 ppm).

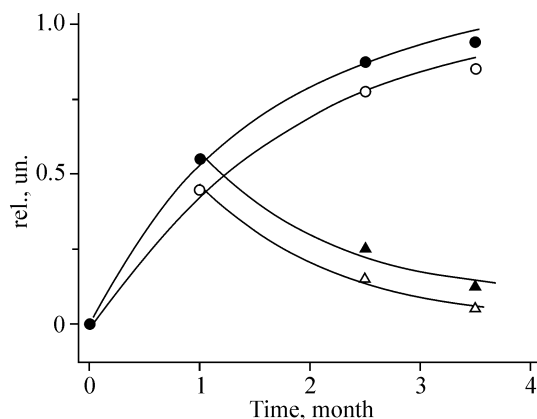


Fig. 7. Dynamics of fluorine accumulation in bone tissue under the conditions of fluoride intoxication (●, ○) and fluorine washout during the postfluoride rehabilitation (▲, △). Filled marks denote standard feed, open marks standard feed with the addition of klinoptilolitic enterosorbent. The intensities of NMR spectra are given in the parts of the maximal value.

nanoparticles which are hypothetically separated by organic ligands. The effect of the zeolite is likely to be indirect in this case and connected with the increase in hydration of tissues, including bone tissue, inducing vacuolation. These processes can promote the “mechanical” widening of escape routes for bioinorganic supramolecular particles, including CaF_2 and MgF_2 , from the parts of bone tissue affected with fluorine followed by their excretion through the system of renal tubules.

DISCUSSION

The instability of small (nanosized) particles, for which, as a rule, rotational diffusion effects are typically observed, is very well-known from studies of the crystal growth of inorganic substances from oversaturated solutions. Theoretical estimates show [17] the existence of a definite critical size. Any smaller crystal “nucleus” dissociates and passes into solution. Above the critical size the “nucleus” can grow indefinitely and turn into a macrocrystal. In view of this, it is worth asking as to whether, under the specific conditions of bone tissue, there is a mechanism that maintains CaF_2 and MgF_2 nanoparticles at a certain size.

Some evidence that such a specific mechanism exists is contained in the data given above for the growth of pure fluoroapatite in bone tissue during fluoride intoxication. It is clear from qualitative considerations that this growth cannot be the result of the simple exchange reaction $\text{F} \leftrightarrow \text{OH}$ on the surface of the initial fluoroapatite because mixed (F, OH)-apatites are not observed under the conditions of fluoride loading. This conclusion is also consistent with a detailed physical-chemical analysis of the apatite structure [18] and the equilibrium conditions in the fluoroapatite–hydroxylapatite system [19-21]. Thus it is necessary to assume that a stage of template formation of F-apatite particles on some organic carrier, or “pattern,” with further stacking of ready particles on the growing bone tissue surface, precedes the epitaxial growth of fluoroapatite on the surface of initial hydroxyapatite. A hypothetical organic carrier could be specific in its action such that the OH-group is excluded from embedding into the forming F-apatite block.

It is possible to envisage that the same (or a structurally close) carrier provides the pattern for the formation of CaF_2 and MgF_2 fluoride particles. In this case the limits on the sizes of CaF_2 and MgF_2 nanoparticles result not from their own properties per se, but by the effects of template “walls” that permits not only the isolation of the given nanoparticles, but also their removing from the organism. The chemical nature of these templates could be similar to a known protein —

amelogenin [18] — and the mechanism related to that of the formation mechanism of hydroxylapatite nanospheric particles of solid enamel. The molecular weight of amelogenin is approximately 20,000 and the size of its spherical subunits is approximately 40-80 Å. The hydrophilic “tail” of this protein would lead to the “anchoring” and uniaxial rotation of nanoparticles. This is all consistent with the conclusions obtained above, though the nature of the organic templates for bone tissue still remains unclear.

CONCLUSION

We have examined the effects of fluoride intoxication on bone tissue. As we have mentioned, the average fluorine content in living organisms ($\sim 10^{-6}$ ppm, or 1 ppm) is 200 times smaller than the average fluorine content in soil ($\sim 2 \cdot 10^{-4}$) [1]. The lower content in living organisms may indicate the existence of a specific active molecular mechanism of fluorine excretion. We have suggested that this mechanism could involve the formation of bioinorganic supramolecular complexes of specific proteins with CaF_2 and MgF_2 nanoparticles in bone tissue and their further removal from the organism through the renal tubule system. In this view, fluorosis etiology as a systemic disease can be attributed to both excessive (or concentrated) toxicant intake from the surrounding environment and the reduction of the natural function of active removal of fluorides or its damage as a result of infectious or other diseases. The existence of a mechanism for the active removal of fluorides is confirmed by the promoting effect of zeolitic food supplements at the rehabilitation stage, in which direct interaction of zeolite and HF in gastrointestinal tract is excluded. Our general approach using data relating to the structural chemistry of fluorine should be helpful in the development of effective novel techniques and methods for the prevention and treatment both of fluorosis and other bone tissue diseases. The results should also be useful for the development of improved methods for the diagnosis and characterization of diseases caused by excessive fluorine intakes by organisms.

In conclusion, the authors thank V. V. Bakakin for valuable remarks and A. Slobodyuk for their help in recording NMR spectra. This work was supported by RFBR grant No. 05-03-32263.

REFERENCES

1. T. L. Vischer, in: *Fluoride in Medicine*, H. Huber (ed.), Switzerland, Bern (1970).
2. N. D. Priest, in: *Trace Metals and Fluoride in Bones and Teeth*, F. L. van De Vyver (ed.), CRC Press, Boca Raton, FL (1990).
3. C. Christiansen, *Osteoporosis 1990, 3rd Intern. Symp. on Osteoporosis*, K. Overgaard (ed.), Copenhagen, Denmark, Osteopress, Copenhagen (1990).
4. A. H. Siddiqui, *Fluoride*, **3**, 91-96 (1970).
5. Z. Bo, *Envir. Geochem. Health*, **25**, 421-431 (2003).
6. J. Cao, *Food Chem. Toxicol*, **41**, 535-542 (2003).
7. T. Kumio and S. Shiro, *Fluoride*, **24**, No. 2, 62-69 (1991).
8. *Department of Health and Human Services [DHHS], Review of Fluoride: Benefits and Risks. Report of the Ad Hoc Subcommittee on Fluoride*, Washington, DC (1991).
9. C. Bryson, *The Fluoride Deception*, Seven Stories Press (2004).
10. S. P. Gabuda, Yu. V. Gagarinskyi, and S. A. Polischuk, *NMR in Inorganic Fluorides* [in Russian], Atomizdat, Moscow (1978).
11. N. Gelman and R. F. Code, *J. Magn. Res.*, **96**, No. 2, 290-301 (1992); *Solid State NMR*, **14**, 191-201 (1999).
12. A. Ueki, *Immunology*, **82**, 332-335 (1994).
13. S. P. Gabuda, S. G. Kozlova, and N. K. Moroz, *Inventions*, No. 3, 130-132 (1996).
14. I. A. Belitskiy., S. P. Gabuda, A. V. Gorbunov, et al., *The Quantitative Determination of Minerals Using the NMR Method*, Preprint № 10, UIGGM, Siberian Division, Russian Academy of Sciences, Novosibirsk (1988).

15. U. Haeberlen, "High Resolution NMR in Solids: Selective Averaging," Adv. Magn. Reson. Supplement 1, Academic Press (1976).
16. C. D. Martin, S. Chaudhuri, C. P. Gray, and J. B. Parise, *Am. Mineralog.*, **90**, 1522-1533 (2005).
17. L. D. Landau and E. M. Lifshitz, *Static Physic* [in Russian], Fizmatgiz, Moscow (1970).
18. J. C. Elliott, *Structure and Chemistry of the Apatites and Other Calcium Orthophosphates*, Elsevier, Amsterdam (1994).
19. S. Mann, *Biomineralization: Principles and Concepts of Bioinorganic Materials Chemistry*, Oxford University Press, Oxford (2001).
20. T. G. Cooper and N. H. de Leeuw, *J. Mat. Chem.*, **14**, 1927-1932 (2004).
21. N. H. De Leeuw, *Phys. Chem. Chem. Phys.*, **4**, 3865-3870 (2002).